*Supplementary material*

# Prefrontal Cortex Activation While Walking Under Dual-Task Conditions in Stroke: A Multimodal Imaging Study

Emad Al-Yahya, PhD; Helen Dawes, PhD; Heidi Johansen-Berg, DPhil; Udo Kischka, MD; Mojtaba Zarei, MRCP; Janet Cockburn; PhD

*Supplementar methods*

***Experiment 1: PFC activation while walking***

*Participants*

Nineteen individuals with chronic stroke (2 females and 17 males, mean age = 59.61 ± 15.03 years) and 20 healthy controls (8 females and 12 males, mean age = 54.35 ± 9.38 years) volunteered for participation in the study. Detailed description of stroke participants is provided in Table S1. Inclusion criteria for the stroke group were: 1) more than 6 months after stroke, confirmed by CT or MRI scan of the brain and medically stable; 2) able to walk a minimum period of 5 min with or without mobility aids; 3) no cognitive, sensory or psychological impairments precluding full engagement with experimental paradigm; and 4) 18 or more years old and were able to consent for participation in this study. Healthy participants did not have a history of neurological and psychiatric illness, were native English speakers, with normal or corrected to normal vision.

The study was approved by the local NHS Research Ethics Committee (Registration No: 08/H0606/55) and all participants gave their informed consent to participate in the study according to the Declaration of Helsinki (2008).

*Experimental procedure*

At baseline, a battery of behavioural tests was administered to assess the level of functional abilities in stroke participants, including; the Short Orientation–Memory–Concentration test (SOMCT) test [1], the Barthel ADL Index [2], the Berg Balance Scale (BBS) [3], the modified physical activity scale of the elderly (PASE) [4], and the 10-metre walk test [5].

Each participant then completed two walking trials on a treadmill (Woodway ELG 75, Germany), under single- and dual-task conditions. Several practice trials were used to familiarize participants with the treadmill and to determine their self-selected walking speed, which was maintained for the single- and dual-task walking. Participants were asked to find a "natural comfortable walking speed" by adjusting the treadmill speed control themselves, or with help if needed.

Each walking task consisted of a 30s task period repeated five times and alternated with rest periods. To avoid anticipation of the start of task periods, the duration of rest period ranged from 25 to 45 s in a pseudo-random order. During the single-task blocks, participants were asked to walk naturally. During the dual-task blocks, participants were asked to count backward in sevens from a random number between 291 and 299. The instructions before dual-task blocks were standardised for all participants to "walk and count out loud as quickly and accurately as possible". Before each walking block, participants were given a verbal instruction; for the single-task blocks the instruction was "in 1, 2, 3 go", for the dual-task block the instruction was "the number is 297 (for example) and you can start now". Instructions were started 3 – 4 s before the walking blocks and synchronised with the treadmill start (Figure S.1). During walking serial responses were verbalised by participants and each response was recorded; rate (figures enumerated per time) and accuracy (percentage of correct answers) were used to measure cognitive task performance.

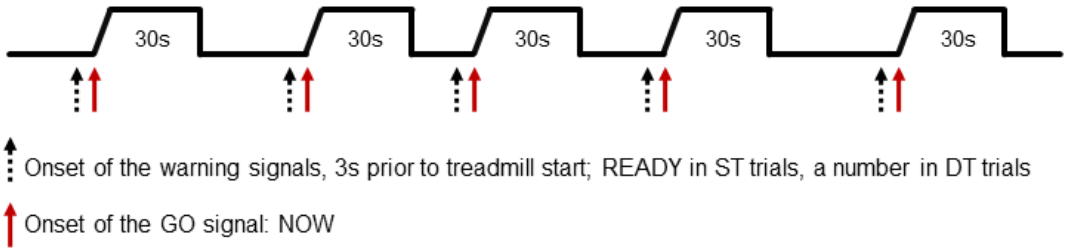


**Fig S.1:** Experimental procedure; walking tasks paradigm

*Data acquisition*

The present study used NIRS allowing spatial localization of brain activation by measuring task-related hemodynamic responses[6, 7]. PFC activation was measured with the Oxymon Mk III system (Artinis Medical Systems, The Netherlands). The multichannel system uses two wavelengths at 782 nm and 859 nm to estimate relative changes in the concentration of oxygenated (oxy-Hb) and deoxygenated (deoxy-Hb) haemoglobin respectively. Two identical plastic holders consisting of four optodes each (2 sources, 2 detectors) in a 4-channel arrangement with an interoptode separation of 30 mm were placed on each participant's forehead. The arrays were custom-built and used spring-loaded optodes as they are more stable. The holders covered the area linking Fp1, F3 and F7 and the area linking Fp2, F4, and F8 according to the international 10-20 EEG electrode system, which corresponds to the left and the right PFC respectively [8]. Considering that the spatial resolution of NIRS is in the order of a few centimetres [7], therefore, two regions of interest (ROI) were defined; left and right PFCs, covered by channels 1, 2, 3, 4 and 5, 6, 7, 8 respectively.

Optical signals were continuously sampled at 10 Hz, and stored according to their wavelength and location, resulting in values for changes in the concentration of oxy-Hb and deoxy-Hb from each of the 8 channels. Optical data were used to quantify task-related changes of oxy-Hb and deoxy-Hb based on the modified Beer-Lambert law [9].

Spatiotemporal gait parameters were assessed using an inertial measurement unit comprising of a tri-axial accelerometer, gyroscope and magnetometer (MTx, Xsens, Netherlands) that

was attached over the skin of the 4th lumbar vertebra [10], corresponding to the participant's projected centre of mass (CoM) during walking [11]. Vertical acceleration, speed and position measurements of the CoM were obtained by transposing acceleration from the object to the global system [10]. Gait data was continuously sampled at 100 Hz. Systematic blood pressure was measured (Dinamap, GE Healthcare, USA) at the beginning and after the end of each trial. There were no significant changes in systematic blood pressure due to the walking.

*Data processing*

NIRS data processing was performed using the OxySoft software (version 2.1.6) provided with the Oxymon Mk III system. NIRS signals were visually inspected for artefacts such as missing or noisy signals. Motion artifacts were defined as sudden changes in the amplitude of the NIRS signals (oxy-Hb and deoxy-Hb) that were much larger than the expected changes and that appeared in several channels, while missing signals were characterized by flat-line appearing traces of oxy-Hb and/or deoxy-Hb changes. Blocks with artefacts were excluded from the analysis. To remove high frequency noise such as cardiac pulsation, NIRS signals were then low-pass filtered at a 0.67 Hz cut off frequency using the Matlab software.

In order to account for slow drifts in the measurements, individual NIRS signals were baseline-corrected on a block-by-block basis by subtracting the mean intensity of the 5 s preceding trial onset (i.e. last 5 s of rest block) from the overall task block. For each task, signals from the five repeats (i.e. 5 s before onset to 5 s post task) were averaged. For the analysis of brain activation, the middle 10 s of task block was selected and the average concentration changes within this time window was used for further analysis.

To identify channels exhibiting task-related activation, average concentration changes were compared to zero (i.e. the average baseline-corrected activation) by means of t-tests for all tasks, and active channels were defined as statistically different relative to baseline. Data from active channels were used for subsequent analyses as described below.

Inertial measurement unit (IMU) data analysis was performed using a customised program written in LabVIEW 8.5 (National Instruments, Austin, USA) [10]. Initially, relative vertical CoM position was derived by double integrating translatory acceleration. Then, CoM relative position was used to estimate spatiotemporal gait parameters according to the inverted pendulum gait model, where the CoM is vaulted over the lower limb acting as a rigid body during the stance phase of a given gait cycle [12, 13].

*Statistical analysis*

Statistical analysis was performed using SPSS 17.0 (SPSS, Inc.). Counting backward performance was assessed by rate (enumerated numbers per block) and accuracy (percentage of correct answers). Spatiotemporal gait data were analysed by conducting a mixed-design ANOVA with task (2 levels; single and dual) as the independent variable for each measure separately (i.e. step time, cadence, step length, and stride length), and participants' group (stroke vs. control) as the between-subject factor.

For the NIRS data statistical analysis, the average of combined activated channels was calculated for each task and region of interest. Data from all participants were analysed by conducting a mixed-design ANOVA with task (2 levels; ST-walking and DT-walking) and ROI (2 levels; left and right) as the independent within-subjects variables for oxy-Hb and deoxy-Hb separately, while participant group (stroke vs. control) was the between-subjects factor. Whenever Mauchly's test indicated that the assumption of sphericity had been violated for a main effect, Greenhouse–Geisser estimates were used to correct degrees of freedom and results of their statistics are reported.

For all statistical tests, alpha level was set at .05 a *priori*, and SPSS-generated Bonferroni adjusted *p*-values are quoted. A Spearman's Rank Order correlation was run to determine the relationship between DT-related changes in PFC activation (i.e. oxy-Hb concentration) and

those changes in spatiotemporal gait measures. The strength of these correlation coefficients was compared between patients and controls using Fisher's r to z transform. To account for baseline differences in single-task performance, dual-task-related changes in both PFC activation and spatiotemporal gait measured was calculated as relative changes by the following formula [14]:

$$DTchange = \frac{(DT - ST)}{ST} \times 100$$

***Experiment 2: multimodal imaging of PFC while simulated walking***

Nine individuals with chronic stroke (all males, mean age = 66.2 ± 8.3 years; mean time since onset = 26.4 ± 16.6 months), who participated in the previous study, and 10 healthy controls (4 females and 6 males, mean age = 56.2 ± 9.5 years), 8 of them participated in the previous study, volunteered for participation in the study. Details of stroke participants' characteristics are shown in Table S.1.

For stroke participants, and in addition to the previously mentioned inclusion criteria, they had to be able to perform a bilateral reciprocal feet tapping task. The study was approved by the local NHS Research Ethics Committee (Registration No: 09/H0606/55) and all participants gave their informed consent to participate in the study according to the latest version of the Declaration of Helsinki (2008).

**Table S.1** Stroke patients' characteristics

| Subject | Sex | Age | TSO | Lesion site | BI | 10-m |
|---|---|---|---|---|---|---|
| 1 | M | 72 | 12 | Insular infarct (L) | 20 | 17.5 |
| 2 | M | 60 | 24 | Lacunar infarct (L) | 19 | 8.5 |
| 3 | M | 58 | 67 | Basal ganglia (haemorrhagic) (L) | 19 | 9.5 |
| 4 | M | 62 | 15 | Putamen (L) | 20 | 8 |
| 5 | M | 79 | 16 | Temporal lobe (R) | 20 | 11.5 |
| 6 | M | 57 | 20 | Putamen haemorrhage (R) | 19 | 15.3 |
| 7 | M | 71 | 28 | Lacunar infarct (R) | 20 | 12 |
| 8 | M | 61 | 23 | Lacunar infarct (L) | 18 | 9.5 |
| 9 | M | 76 | 33 | Lacunar infarct (R) | 20 | 13 |

**TSO**= time since onset in months; **BI**=Barthel Index scores; **L**= left; **R**=right; **10-m**= time taken in seconds to walk a 10 m long distance

*Experimental procedure*

Participants were given full verbal instructions on the tasks before entering the scanning room. Once instructions were clearly understood, participants were trained and given enough practice to ensure that they were able to carry out the protocol successfully. The two tasks were; 1) counting backward covertly in threes or twos (depending on participant's ability) from a given two digit number; and 2) reciprocal feet movement in response to each visual cue.

Four experimental conditions required participants to perform a single task, dual tasks or rest without movement or counting. The conditions were; A) single task, counting only; B) single task, feet movement only; C) dual task, counting and feet movement concurrently; and D) rest.

The paradigm consisted of 30s blocks of the tasks in ABDC cycle (Figure S.2). The cycle was repeated 6 times, giving a total paradigm length of 12 min. Task performance was paced by a flashing symbol projected onto a screen at the foot of the scanner tube. A different symbol was used for each of the four conditions. So, participants were instructed to count

back one digit (condition A), move feet once (condition B), or both (condition C), each time a symbol flashed on the screen. Each 30s block was preceded by an instruction screen (e.g. A: “count back from 97”, B: “move your feet”, C: “move your feet & count from 98”, D: “rest”). For each counting block a different number was given to participants at the starting point.

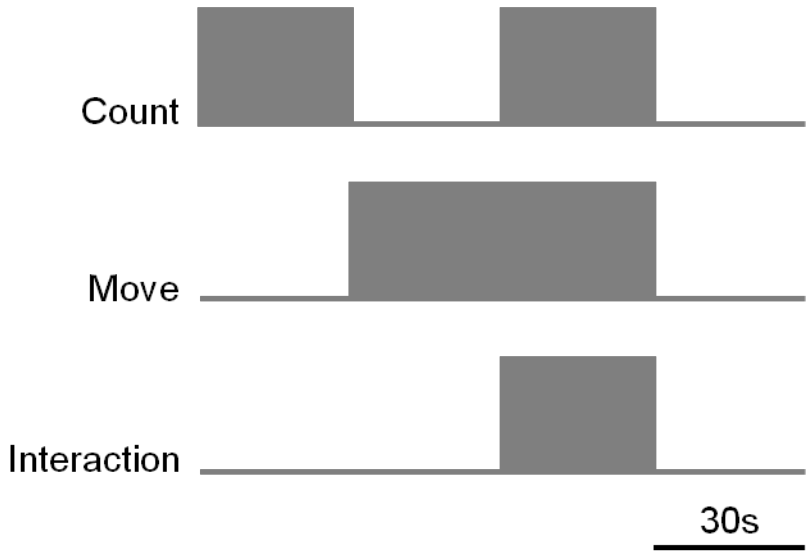


**Fig S.2:** Paradigm design; one ABCD cycle. This cycle was repeated 6 times giving a total paradigm length of 12 min. The top row indicates when participants engaged in the counting task, the second row indicates when participants were moving their feet and the third row indicates the interaction between the two (i.e. blocks when the two tasks were performed simultaneously).

Reciprocal bilateral feet movements were restricted to one degree of freedom (extension-flexion at the ankle joint), using a custom-built plastic apparatus (Figure S.3). Participants were required to take off their shoes, and their feet were secured firmly to the apparatus using flexible traps.

As movement rates are highly variable between participants, the rate of the moving cue presentation was set individually for each participant. First, during the training session,

participants were asked to move their feet using the apparatus for 30s, and the number of foot movements was determined. A cueing rate for the use in the scanner was then chosen that presented 80% of the movement rate outside the scanner. The same cueing rate was used for counting; if participants could not match the movement rate while counting backward by 3s, different numbers were used so that they were able to perform the counting task (i.e. counting back by 2s or 1s).

To assess whether or not participants were counting in the single and dual task conditions (i.e. conditions A and C), participants were presented with a number by the end of the block (e.g. “the number is 71”), and participants were asked to press a ***yes*** button if the number matched the one they reached (i.e. correct answer) or a ***no*** button if the presented number did not match the one they reached (i.e. wrong answer). The correct and wrong answers were counterbalanced (i.e. 6 (3 single and 3 dual) blocks ended with wrong answers and 6 with correct answers).

To control for the answering element of the counting task, by the end of the movement blocks (condition B) participants were presented with a screen that showed an arrow pointing to either the left or the right, and the words left or right written under the arrow. Participants were asked to press ***yes*** if the word matched the direction of the arrow or ***no*** if the word did not match the direction of the arrow.

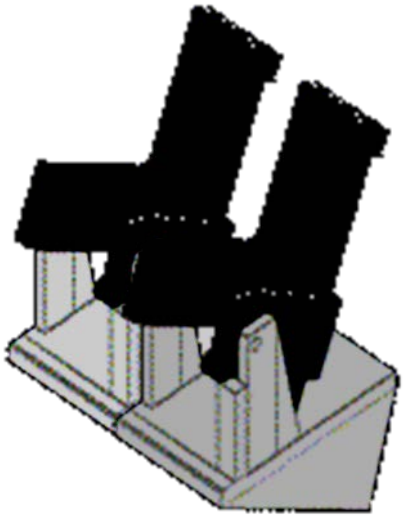

**Fig S.3:** Feet movement constraint apparatus, the footrests rotate to allow extension-flexion movements at the ankle joints.

Participant compliance with the movement task was confirmed by a potentiometer fitted to the feet apparatus (Figure S.3). The signals from the potentiometer as well as a record of stimulus presentation and button press were collected and analysed off line.

*Image acquisition*

Imaging data were acquired using a 3.0-T TrioTim syngo (Siemens, Erlangen, Germany) MRI system. A total of 256 T2*-weighted blood-oxygen-level-dependent (BOLD) sensitive echo planar imaging (EPI) images were acquired during task performance (45 axial slices per volume, TR=3000 ms, TE=30 ms, matrix=64 x 64, in-plane resolution=3 x 3 $mm^2$, flip angle=87°). A $T_1$-weighted anatomical image was also acquired (TR= 3000 ms, TE= 4.71 ms, TI (inversion time) = 1100 ms, flip angle 8°, FOV 256 X 256, matrix = 256 X 256).

Simultaneously, PFC activation was measured, as task-related change of oxy-Hb and deoxy-Hb, with the Oxymon Mk III system (Artinis Medical Systems, The Netherlands) as described in section 6.2.4, using an MRI compatible NIRS probe. NIRS data acquisition was synchronized with the fMRI measurements using a trigger from the MRI scanner.

*Data analysis*

Image analysis was carried out using tools from the FMRIB Software Library (Analysis group, FMRIB, Oxford, UK, www.fmrib.ox.ac.uk/fsl).

The following pre-statistical processing was applied: Motion correction using MCFLIRT [15]; non-brain removal using BET [16], spatial smoothing using a Gaussian kernel of 5 mm full-width half maximum; mean based intensity normalisation; non-linear high-pass temporal filtering (Gaussian-weighted, least squares straight line fitting with sigma = 120 seconds); fieldmap unwarping using FUGUE [17]. In order to investigate the possible presence of unexpected artefacts or activation, ICA-based (independent component analysis) exploratory data analysis was carried out using MELODIC [18] for each individual data set. Components whose temporal or spatial profiles reflected artifacts rather than activity related changes were removed from further analysis [19].

Statistical analysis of the images was performed in two stages. The first level (within subject) analysis was carried out using FEAT with local autocorrelation correction [20] to produce effect size images of task related activity versus rest and the positive interaction between the two tasks. At this stage, single tasks of counting and moving alone were modelled as two separate event types, while the DT was modelled as the positive interaction between the two single tasks. The two original EVs (i.e. count and move) were first modelled, and then an interaction EV (i.e. DT), which would be 'up' when both of the original EVs were 'up' [21]. Therefore, the interaction EV modelled the extent to which the response to count + move was greater than the sum of count-only and move-only (Figure S.4). This was done by selecting **Interaction** in FEAT then the dual-task EV was used to create a third EV from two existing EVs, to model the nonlinear interaction between two different conditions. A contrast of [0 0 1] showed this measure.

Registration of fMRI images to high-resolution structural images and into standard space (MNI template [22]) was carried out using FLIRT [15].

Higher-level (i.e. group) analysis was carried out on the resulting aligned images using mixed effects with automatic outlier detection and de-weighting [23] to calculate group average patterns of task related activity and to test for correlations between DT-related activity (i.e. positive interaction contrast) and behavioural DT-changes (calculated as described in section 7.2.5). The group Z (Gaussianised *T*) statistic images were thresholded using clusters determined by Z>2.3 and a (corrected) cluster significance threshold of $P=0.01$[24]. Clusters showing a correlation with behavioural DT-changes were masked by the group average DT-related activity to identify DT-related areas where increased activity correlated with increased behavioural DT-changes.

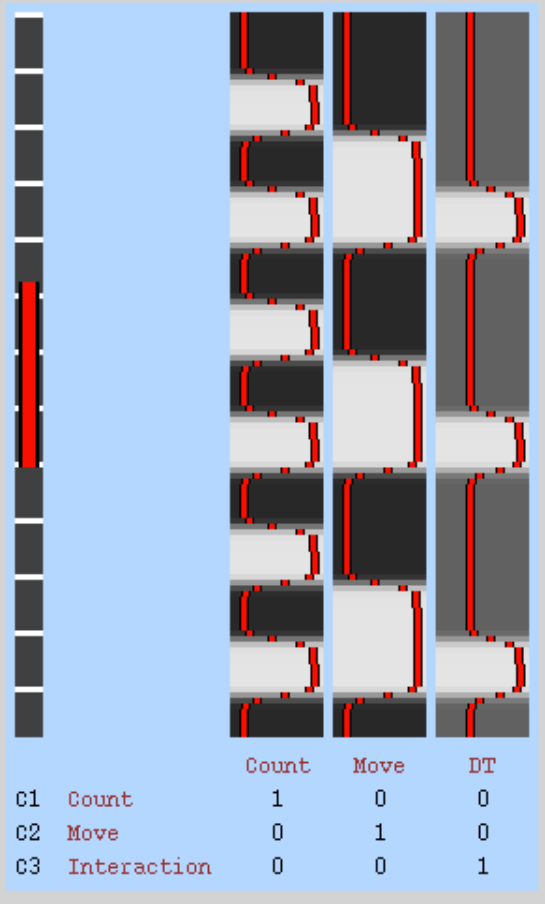

**Fig S.4:** Design matrix of modelling the nonlinear interaction between the two conditions. The first two EVs model the separate stimuli (i.e. count and move), whilst the third models their interaction, i.e. accounts for 'extra' response when both stimuli are applied together.

This resulted in Z statistic images for the main effects of counting and of movement and for the interaction between the two tasks. Areas showing a positive interaction were more active in the dual task condition than the sum of the two single task conditions. The positive interaction was of prime interest, as this would include areas that are exclusively related to the dual task performance. Finally, Featquery was used to estimate percent signal change of the masked group average DT-related areas that correlated with increased behavioural DT-changes.

For each contrast, thresholded significant clusters are reported according to their coordinates in the MNI standard space and the centre-of-gravity (COG) and number of activated voxels for each cluster. All images are shown in radiological convention in which the left side of the image is the right side of the brain.

For NIRS measurement, signals were pre-processed as described before and PFC activations were assessed statistically by comparing average concentration changes of oxy-Hb and deoxy-Hb within trials (the time between 6 - 16 s after stimulus onset) between the two groups and experimental conditions by using mixed design repeated-measures ANOVAs (SPSS 17).

*Supplemental results:*

**Table S.2.** Correlation analyses of the relationship between DT-related changes in PFC activation and gait measures

| | | **Left PFC** | | **Right PFC** | |
|---|---|---|---|---|---|
| | | Stroke | Control | Stroke | Control |
| **Step time** | $r_s$ | 0.747 | -0.159 | 0.867 | -0.209 |
| | ***P*-value** | **0.000** | 0.502 | **0.000** | 0.376 |
| **Cadence** | $r_s$ | -0.528 | 0.152 | -0.633 | 0.183 |
| | ***P*-value** | **0.02** | 0.523 | **0.004** | 0.439 |
| **Step length** | $r_s$ | 0.560 | 0.192 | 0.681 | 0.215 |
| | ***P*-value** | **0.013** | 0.416 | **0.001** | 0.362 |
| **Stride length** | $r_s$ | 0.535 | -0.048 | 0.656 | -0.137 |
| | ***P*-value** | **0.018** | 0.842 | **0.002** | 0.566 |

**Table S.3** Activated clusters in random effects group analysis of movement versus rest

| Group Contrast | Region | Side | Voxels | MNI Coordinates (COG) | | |
|---|---|---|---|---|---|---|
| | | | | X | Y | Z |
| **Control (mean)** | | | | | | |
| | Brain-Stem | L | 5696 | 12 | -21 | -17 |
| | Lingual G | L&R | 2313 | 0 | -80 | 9 |
| | Precentral G | L&R | 2155 | 0 | -27 | 60 |
| | Planum Temporale | L | 522 | -49 | -33 | 16 |
| | Temporal Pole | L | 468 | -39 | 7 | -35 |
| | Crus I | R | 395 | 48 | -58 | -25 |
| | Crus I | L | 184 | -39 | -52 | -30 |
| | Cingulate G | L | 159 | -4 | -38 | 23 |
| **Stroke (mean)** | | | | | | |
| | Vermis VI | R | 3202 | 4 | -65 | -25 |
| | Inferior Temporal G | R | 935 | 45 | -10 | 9 |
| | Putamen | R | 787 | 27 | 8 | -25 |
| | Postcentral G | L&R | 618 | 1 | -33 | 63 |
| | Precuneous C | R | 351 | 3 | -72 | 40 |
| | Lateral Occipital C | L | 325 | -37 | -84 | 2 |
| | Thalamus | L | 314 | -13 | -5 | 5 |
| | Angular G | L | 241 | -43 | -59 | 43 |
| | Cerebellum (VIIb) | R | 207 | 3 | -72 | -50 |
| | Palnum Temporale | L | 197 | -54 | -33 | 19 |
| | Occipital Pole | R | 178 | 13 | -100 | -3 |

**L**= left; **R**= Right

**Table S.4** Activated clusters in random effects group analysis of positive interaction between counting and movement

| Group Contrast | Region | Side | Voxels | MNI Coordinates (COG) | | |
|---|---|---|---|---|---|---|
| | | | | X | Y | Z |
| **Areas showing positive interaction in the control group** | | | | | | |
| | Occipital pole | R | 594 | 16 | -92 | -7 |
| | Occipital pole | L | 471 | -20 | -92 | -13 |
| **Areas showing positive interaction in the stroke group** | | | | | | |
| | Superior Frontal G | L&R | 1052 | -5 | 55 | 25 |
| | Caudate | L | 893 | -13 | 26 | -8 |
| | Inferior Temporal G | L | 783 | -49 | -7 | -31 |
| | Superior Frontal G | L | 287 | -17 | 12 | 52 |
| | Inferior Temporal G | R | 260 | 43 | -5 | -40 |
| **Areas showing increased positive interaction in control compared to stroke** | | | | | | |
| | Occipital pole | L&R | 989 | 6 | -92 | -7 |
| | Crus II | R | 353 | 1 | -81 | -32 |
| | Angular G | R | 243 | 56 | -46 | 31 |
| | Inferior longitudinal F (WM) | L | 147 | -32 | -41 | 14 |
| | Precuneus C | R | 145 | 17 | -55 | 30 |
| | Postcentral G | L | 111 | -53 | -7 | 19 |
| | Inferior Temporal G | R | 110 | 51 | -44 | -12 |
| **Areas showing increased positive interaction in stroke compared to control** | | | | | | |
| | Inferior Temporal G | L | 767 | -49 | -7 | -31 |
| | Inferior Temporal G | R | 430 | 39 | -8 | -38 |
| | Superior Frontal G | L | 405 | -20 | 5 | 54 |
| | Superior Frontal G | R | 393 | 17 | 17 | 53 |
| | Cingulate G | L&R | 280 | -4 | 25 | -6 |
| | Precentral G | R | 238 | 37 | -10 | 51 |
| **Areas showing positive correlation between DT-activation and DT-cost (Stroke)** | | | | | | |
| | Inferior Temporal G | L | 811 | -48 | -6 | -32 |
| | Inferior Temporal G | R | 280 | 43 | -5 | -41 |
| | Cingulate G | L | 249 | -11 | 28 | -9 |
| | Middle Frontal G | L | 203 | -29 | 46 | 27 |

**L**= left; **R**= right; **G**= gyrus; **DT**= dual-task; **F** = fasciculus; **WM** = white matter

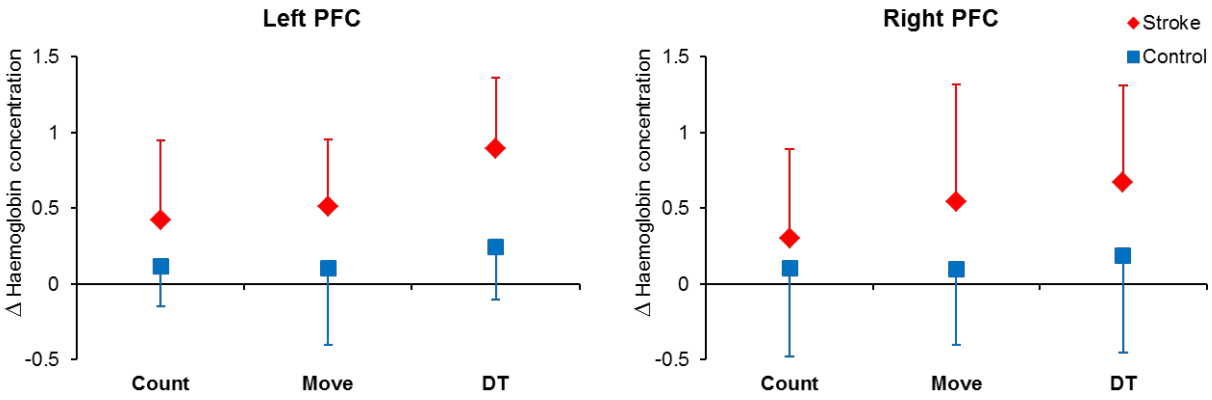


**Fig S.5:** Group data (mean ± SD) of task-related changes in oxy-Hb concentrations in PFC during counting, ankle movement and dual-task (DT).

## References


1. Katzman R, Brown T, Fuld P, Peck A, Schechter R, Schimmel H. Validation of a short orientation-memory-concentration test of cognitive impairment. *Am J Psychiatry*. 1983;140:734-739
2. Wade D, Collin C. The barthel adl index: A standard measure of physical disability? *International Disability Studies*. 1988;10:64-67
3. Berg K, Wood-Dauphinee S, Williams J, Maki B. Measuring balance in the elderly: Validation of an instrument. *Can J Public Health*. 1992;83:S7-S11
4. Washburn RA, Smith KW, Jette AM, Janney CA. The physical activity scale for the elderly (pase): Development and evaluation. *Journal of Clinical Epidemiology*. 1993;46:153-162
5. Wade D. *Measurment in neurological rehabilitation* Oxford: Oxford University Press; 1992.

6. Lloyd-Fox S, Blasi A, Elwell CE. Illuminating the developing brain: The past, present and future of functional near infrared spectroscopy. *Neuroscience & Biobehavioral Reviews*. 2010;34:269-284

7. Huppert TJ, Diamond SG, Franceschini MA, Boas DA. Homer: A review of time-series analysis methods for near-infrared spectroscopy of the brain. *Appl. Opt.* 2009;48:D280-D298

8. Leff DR, Elwell CE, Orihuela-Espina F, Atallah L, Delpy DT, Darzi AW, Yang GZ. Changes in prefrontal cortical behaviour depend upon familiarity on a bimanual co-ordination task: An fnirs study. *NeuroImage*. 2008;39:805-813

9. Delpy D, Cope M, Zee P van der, Arridge S, Wray S, Wyatt J. Estimation of optical pathlength through tissue from direct time of flight measurement. *Physics in Medicine and Biology*. 1988;33:1433

10. Esser P, Dawes H, Collett J, Howells K. Imu: Inertial sensing of vertical com movement. *Journal of Biomechanics*. 2009;42:1578-1581

11. Kerrigan DC, Viramontes BE, Corcoran PJ, LaRaia PJ. Measured versus predicted vertical displacement of the sacrum during gait as a tool to measure biomechanical gait performance. *American Journal of Physical Medicine & Rehabilitation.* 1995;74:3-8

12. Zijlstra W. Assessment of spatio-temporal parameters during unconstrained walking. *European Journal of Applied Physiology*. 2004;92:39-44

13. Gonzalez RC, Alvarez D, Lopez AM, Alvarez JC. Modified pendulum model for mean step length estimation. *Engineering in Medicine and Biology Society. 29th Annual International Conference of the IEEE*. 2007:1371-1374

14. Abernethy B. Dual-task methodology and motor skills research: Some applications and methodological constraints. *J Hum Mov Study*. 1988;14:101 - 132

15. Jenkinson M, Smith S. A global optimisation method for robust affine registration of brain images. *Medical Image Analysis*. 2001;5:143-156

16. Smith SM. Fast robust automated brain extraction. *Human Brain Mapping*. 2002;17:143-155

17. Jenkinson M. Fast, automated, n-dimensional phase-unwrapping algorithm. *Magnetic Resonance in Medicine*. 2003;49:193-197

18. Beckmann C, Smith S. Probabilistic independent component analysis for functional magnetic resonance imaging. *IEEE Trans. on Medical Imaging*. 2004;23:137-152

19. Tohka J, Foerde K, Aron AR, Tom SM, Toga AW, Poldrack RA. Automatic independent component labeling for artifact removal in fmri. *NeuroImage*. 2008;39:1227-1245

20. Woolrich MW, Ripley BD, Brady M, Smith SM. Temporal autocorrelation in univariate linear modeling of fmri data. *NeuroImage*. 2001;14:1370-1386

21. Smith S. Overview of fmri analysis. In: Jezzard P, Matthews P, Smith S, eds. *Functional mri an introduction to methods*

Oxford: Oxford University Press

2001:215-227.

22. Collins DL, Holmes CJ, Peters TM, Evans AC. Automatic 3-d model-based neuroanatomical segmentation. *Human Brain Mapping*. 1995;3:190-208

23. Woolrich M. Robust group analysis using outlier inference. *NeuroImage*. 2008;41:286-301

24. Worsley KJ. Statistical analysis of activation images. In: Jezzard P, Matthews P, Smith S, eds. *Functional mri an introduction to moethods*. Oxford: Oxford University Press; 2001:250-270.